Mon. Not. R. Astron. Soc. **324,** L7–L10 (2001)

Coronal Fe IX line intensities and electron density diagnostics

P. J. Storey[1]★ and C. J. Zeippen[2]★

[1]*University College London, Department of Physics and Astronomy, Gower Street, London WC1E 6BT*

[2]*UMR 8631 (associée au CNRS et à l'Université Paris 7) et DAEC, Observatoire de Paris, F-92195 Meudon, France*

Accepted 2001 March 29. Received 2001 March 16; in original form 2000 September 27

ABSTRACT

The relative intensities of the most prominent extreme-ultraviolet lines of Fe IX, seen in the outer atmospheres of the Sun and other stars, have been shown to be inconsistent with the best available atomic data. The density-sensitive Fe IX $\lambda 241.7/\lambda 244.9$ line intensity ratio, for example, yields electron densities in the solar corona that disagree with those obtained from ratios in other ions, particularly at higher densities. We show here that these differences can be largely removed by using newly calculated atomic data, in particular electron impact collision strengths that include pronounced resonance features, and by incorporating a measure of line excitation by collisional excitation and cascading.

Key words: atomic processes – Sun: corona – Sun: flares.

1 INTRODUCTION

The intensity ratio of the Fe IX $3p^5 3d\ ^3P^o_2$–$3p^6\ ^1S_0$ magnetic quadrupole transition at 241.7 Å to the $3p^5 3d\ ^3P^o_1$–$3p^6\ ^1S_0$ intercombination transition at 244.9 Å is of practical interest in solar studies because the two lines lie close in wavelength and are not significantly blended. This makes comparisons of their intensities relatively easy. Feldman, Doscheck & Widing (1978), assuming the solar plasmas to be in a steady state at an electron temperature of 9×10^5K, calculated line intensity ratios as a function of electron density over the density range 10^9–$10^{13}\,\mathrm{cm}^{-3}$, using the electron collision strengths of Flower (1977) and the radiative decay rates of Flower (1977) and Garstang (1969). Feldman et al. (1978) reported that, in the low-density limit, the calculated intensity ratio of the $\lambda\lambda 241.7$ and 244.9 lines is in reasonable agreement with that measured from the whole-Sun spectra of Behring, Cohen & Feldman (1972), and went on to discuss the use of this ratio to determine electron densities above about $10^{10}\,\mathrm{cm}^{-3}$.

Further work was done on the Fe IX atomic model by Haug (1979), who added the effect of cascades from higher energy levels to the original calculation of Feldman et al. (1978). More recently, Fawcett & Mason (1991) reconsidered the atomic data calculations of Flower (1977). Although based on the same computer package, composed of DSTWAW (Eissner & Seaton 1972), JAJOM (Saraph 1970, 1972) and SUPERSTRUCTURE (Eissner, Jones & Nussbaumer 1974), this study included an adjustment of Slater parameters (Fawcett & Mason 1989) using a subroutine in the HFR code of Cowan (1981). Also, a lack of consistency in the level indexing in the work of Flower was corrected. Finally, Mandelbaum (private communication to Feldman 1992) provided a new set of atomic data yielded by the code HULLAC (Oreg et al. 1991), while Liedahl (2000) used the same code to explore the effect of dramatically increasing the number of states in the Fe IX atomic model.

Feldman (1992) reviewed the various sets of atomic data available and drew attention to the much larger electron densities derived from flare spectra using the Fe IX $\lambda 241.7/\ \lambda 244.9$ line intensity ratio compared with those derived from ratios in other ions (Dere et al. 1979; Widing, private communication to Feldman 1992). Feldman (1992) showed, in his fig. 1, that the theoretical $\lambda 241.7/\lambda 244.9$ intensity ratios available so far differ at most by a factor of 2 at high densities, which is not enough to account for the discrepancies. He concludes that the available atomic data are most likely not wrong enough to be the cause of the problem. He then goes on to suggest a possible explanation. In short, the metastable emission lines used in solar plasma diagnostics could be affected by short-lived bursts, and the model of a steady-state plasma could be partly invalid.

More recently, Laming, Drake & Widing (1995) drew attention to the fact that the intensity of the Fe IX $\lambda 171.1$ permitted line is also discrepant with theoretical predictions when compared with both the $\lambda\lambda 241.7$ and 244.9 lines in the *Solar EUV Rocket Telescope and Spectrograph* (*SERTS*) data (Thomas & Neupert 1994), the quiet-Sun spectra of Malinovsky & Heroux (1973), and the star Procyon (Drake, Laming & Widing 1995), all of which show a similar intensity pattern for these lines.

Liedahl (2000) has shown that the discrepancies between the predicted and observed intensity ratios for the density-sensitive lines are significantly reduced if the model atom is increased in size. His model includes electron configurations with valence electron principal quantum numbers $n \leq 4$, with a total of 1067 levels. He states, however, that the most important contributions probably come from the levels of the $3p^4 3d^2$ configuration. We

★E-mail: pjs@star.ucl.ac.uk (PJS); zeippen@obspm.fr (CJZ)

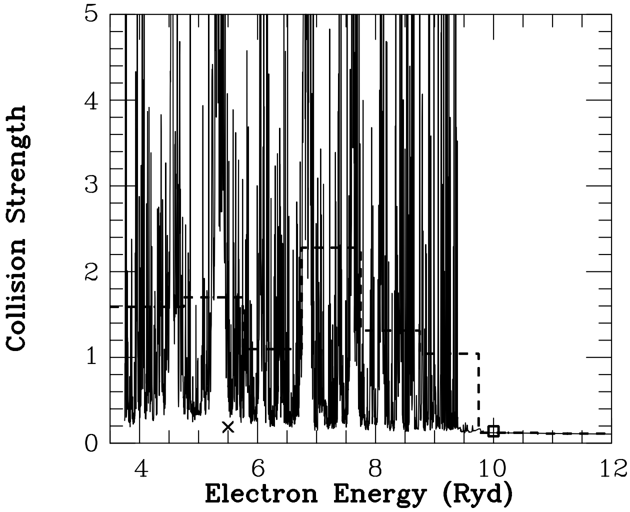

Figure 1. Collision strength for the $3p^5 3d(^3P^o_1)$–$3p^5 3d\ (^3P_2)$ transition. The solid line is from Storey et al. (in preparation). The dashed line shows the same data averaged over 1.0-Ryd intervals. The cross is from the calculations of Flower (1977), while the square is from Fawcett & Mason (1991).

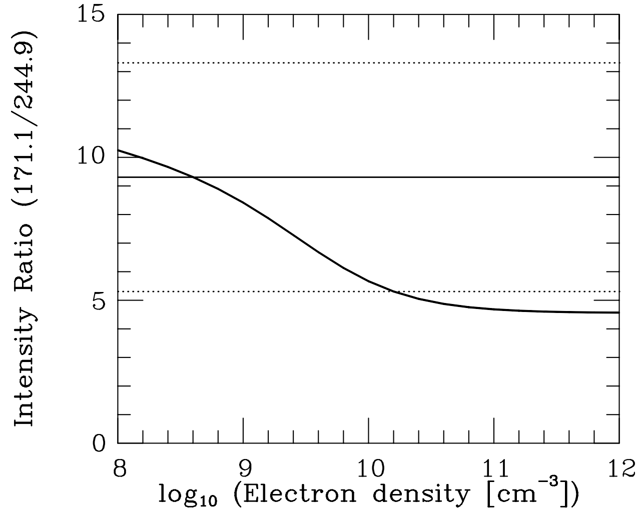

Figure 2. The λ171.1/λ244.9 intensity ratio as a function of electron density at $T_e = 9 \times 10^5$K, derived from the atomic data of Storey et al. (in preparation). The solid horizontal line corresponds to the observed ratio from the *SERTS* data of Thomas & Neupert (1994). The dotted lines correspond to the errors on the line intensities quoted by Thomas & Neupert (1994).

note that the collision rates used by Liedahl (2000) do not include resonance effects.

As part of the international collaboration known as the IRON Project (IP: see the general description by Hummer et al. 1993), Storey, Zeippen & Le Dourneuf (in preparation, hereafter referred to as SZL) performed elaborate quantal calculations of the electron impact of Fe IX, allowing in particular for resonance effects in the collisional cross-sections. More information on the IP and a list of papers in the IP series can be found at the URL http://www.usm.uni-muenchen.de/people/arch4/ iron-project.html. The aim of the present Letter is to demonstrate the effect of the new collision rates of SZL on the calculated intensities of the four most prominent lines of Fe IX, the λ241.7 magnetic quadrupole line, the λ244.9 intercombination line, the λ171.1 resonance line and the further intercombination line at 217.1 Å.

2 THE METHOD

The computer codes used by SZL to produce new collisional and radiative rates for lines in Fe IX are described by Hummer et al. (1993). They are the RMATRX (Berrington, Eissner & Norrington 1995; Berrington et al. 1987) and SUPERSTRUCTURE (Eissner et al. 1974; Nussbaumer & Storey 1978; Eissner 1991) programs. Technical details will not be repeated here. In the context of the present communication, it is important to underline the fact that, contrary to previous work, the effect of resonances in the collisional cross-sections was taken into account by SZL. It is well known that resonances often cause more or less important enhancements in the calculated effective collision strengths obtained through a convolution with a Maxwellian distribution of electron velocities. The configuration basis set selected by SZL consists of 11 configurations. The scattering calculation itself retains 58 terms and 130 levels in Fe IX. For partial waves up to $l = 15$, a full RMATRX calculation was performed in *LS*-coupling plus the mass and Darwin relativistic corrections, while the higher partial wave contribution was estimated with a Coulomb–Bethe top-up procedure inherited from the Opacity Project (Opacity Project Team 1995, 1996).

The 58 terms of the scattering calculation belong to the five electronic configurations $3p^6$, $3p^5 3d$, $3s3p^6 3d$, $3p^5 4s$ and $3p^4 3d^2$, with the $3p^5 4s$ configuration included only because it is energetically within the $3p^4 3d^2$ configuration. The important observed far-ultraviolet lines arise from transitions between the first and second configurations in this list. The density sensitivity of the λ241.739/λ244.911 ratio arises when the rate of collisional de-excitation of the $3p^5 3d\ ^3P^o_2$ level exceeds the magnetic quadrupole radiative decay rate to the ground level. Collisional de-excitation of the $^3P^o_2$ level can occur to any other level, but the most significant routes are to the ground state and to other levels of the $3p^5 3d$ configuration. We illustrate the importance of resonance contributions to these processes by examining the collision strength for collisional de-excitation to the $^3P^o_1$ level, from where radiative decay is much more rapid. Fig. 1 shows the collision strength for this process as calculated by SZL including resonances, and by Flower (1977) and Fawcett & Mason (1991) without resonances. In the resonance region, the average collision strength from SZL is approximately 10 times greater than the value obtained without resonance effects by Flower (1977). In the energy region above the highest target threshold at 9.91 Ryd we find good agreement with the calculation of Fawcett & Mason (1991). The resonance features seen in Fig. 1 are Rydberg series converging on terms of the $3p^4 3d^2$ electronic configuration, and are especially important because of the strong dipole coupling between the $3p^5 3d$ and $3p^4 3d^2$ configurations and because the non-resonant collision rate for the forbidden $3p^5 3d\ ^3P^o_2$–$^3P^o_1$ transition is relatively small.

The states of the $3p^5 3d$ configuration may also be populated by collisional excitation from the ground state to the states of the $3p^4 3d^2$ configuration followed by radiative decay. We discuss the importance of this mechanism and of resonance enhancements in the final section.

The radiative rates were calculated using the same wave-functions as the ones that describe the Fe IX ion in the collisional calculation. It is possible that more work will be required in order to improve these rates, but their influence on the line intensity ratio

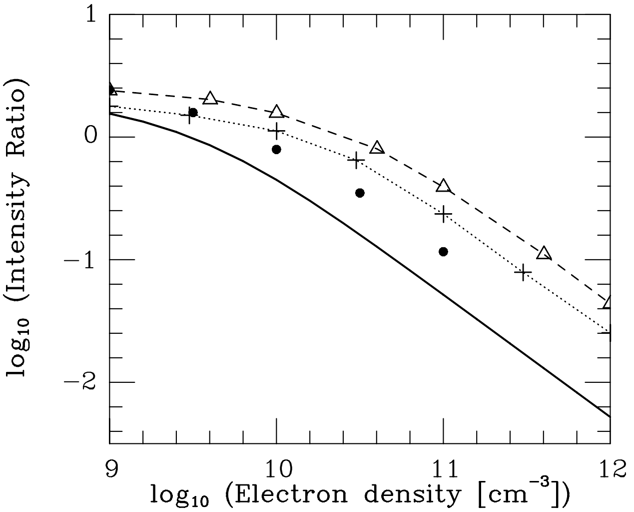

Figure 3. The $\lambda241.7/\lambda244.9$ intensity ratio as a function of electron density at $T_e = 9 \times 10^5$K. The solid line is derived from the atomic data of SZL. Crosses and triangles denote values of the ratio taken from Feldman (1992), which were derived from the atomic data of Flower (1977) and Fawcett & Mason (1991), respectively. The filled circles are taken from the 1067-state model of Liedahl (2000). Note that, using the data of SZL, the critical electron densities for collisional de-excitation of the $3p^53d$ $^3P^o_2$ and $^3P^o_1$ levels are approximately 3×10^9 and 6×10^{16}cm^{-3}, respectively.

examined here is likely to be minor compared with the effect of the new collision rates.

3 RESULTS

3.1 The λ171.1 resonance line

The λ171.1 resonance line is a strong optically allowed transition populated almost entirely by electron collisions from the $3p^6$ $^1S_0$ ground state. As the electron density is increased, the fractional population of the ground state falls as the populations of the metastable levels of the $3p^53d$ configuration rise. As a consequence, the intensity of the λ171.1 line does not rise in direct proportion to the electron density, but rises rather more slowly. By contrast, the λ244.9 intercombination line is populated not just from the ground level but also from all the $3p^53d$ levels, resulting in an intensity that does rise in proportion to the electron density. The $\lambda171.1/\lambda244.9$ line intensity ratio therefore demonstrates a weak density dependence, which is shown in Fig. 2 over the density range 10^8–10^{12}cm^{-3}. In this figure and in all subsequent quoted theoretical ratios an electron temperature of 9×10^5K has been assumed.

From the *SERTS* data of Thomas & Neupert (1994), we find that the observed ratio is 9.3 ± 4.0, corresponding to the theoretical result at $\log N_e = 8.6$, although plainly the error bars are very large. The quiet-Sun spectrum of Malinovsky & Heroux (1973) shows both the $\lambda\lambda$171.1 and 244.9 lines, and, although those authors did not give a measured intensity for the λ244.9 line, from their spectra one can estimate that the ratio is approximately 10, also in good agreement with the current model. These observations are in pronounced disagreement with the theoretical value of 33 quoted by Young, Landi & Thomas (1998) based on the earlier atomic data as incorporated in the CHIANTI data base.

3.2 The $\lambda241.7/\lambda244.9$ line intensity ratio

Theoretical values of this ratio as a function of electron density have been given by Feldman (1992). In Fig. 3 we reproduce two of the curves given by Feldman, derived from the atomic data of Flower (1977) and Fawcett & Mason (1991), in addition to the curve obtained from the atomic data of SZL and from the model of Liedahl (2000). There is reasonable agreement between all three theoretical curves at the lower electron densities, but with the new atomic data the ratio falls more rapidly with increasing electron density, with the current value being smaller by a factor of 7.6 than that obtained by Feldman (1992) from the data of Fawcett & Mason at $N_e = 10^{11}$cm^{-3}, and a factor of 2.3 smaller than that given by Liedahl (2000) at the same density.

We can compare these new theoretical predictions with various observations. From the quiet-Sun spectra of Malinovsky & Heroux (1973), we can estimate the ratio to be 2, consistent with $\log N_e = 8.5$ (not shown in Fig. 3). From the *SERTS* data of Thomas & Neupert (1994), we find a ratio of 1.20 ± 0.56, implying $\log N_e = 9.30 \pm 0.5$ compared with $\log N_e = 10.1$ found by Young et al. (1998) using the data incorporated in CHIANTI. The new value of N_e is in significantly better agreement with densities deduced from diagnostic ratios in other Fe ions from the same *SERTS* data (e.g. Brickhouse, Raymond & Smith 1995). The $\lambda\lambda$241.7 and 244.9 lines were also observed and measured in the *Skylab* data reported by Dere et al. (1979). They found a value of 0.46 for the $\lambda241.7/\lambda244.9$ line intensity ratio in the 1973 December 17 flare, which corresponds to an electron density of 10^{10} cm^{-3} with the new atomic data, while Dere et al. deduced a density five times larger using the atomic data available at the time (Flower 1977).

3.3 The $\lambda217.1/\lambda244.9$ line intensity ratio

In their description of the *SERTS* data, Thomas & Neupert (1994) report a measurement of the λ217.1 line originating from the $3p^53d$ $^3D^o_1$ level. In our present atomic model, this line shows a weak density sensitivity when compared with the λ244.9 intercombination line, with the $\lambda217.1/\lambda244.9$ intensity ratio varying from 0.71 to 0.89 between $\log N_e = 9$ and 12. By contrast, the observed ratio from the *SERTS* data is 0.43 ± 0.24. In view of the good agreement now obtained for the two line ratios discussed above, we believe that the most likely explanation for this discrepancy is the uncertainty in the flux of the λ217.1 line which was measured in second order at λ434.2 in the *SERTS* spectrum. It has been proposed (Brickhouse et al. 1995; Young et al. 1998) that the intensities of lines measured in second order are about a factor of 2 too weak compared with first-order lines. If this were the case, the observed ratio would rise to 0.86, in much better agreement with the new theoretical results.

4 DISCUSSION

What is the cause of the large changes to the $\lambda241.7/\lambda244.9$ intensity ratio derived from the new atomic data? There are two effects at work. First, the effective collision strengths between the metastable levels of the $3p^53d$ configuration are about a factor of 10 larger than in any previous work, as illustrated in Fig. 1. This increases the rate of collisional de-excitation from the important levels for a given electron density. Secondly, there is significant collisional excitation to the levels of the $3p^43d^2$ electron configuration which is followed by cascade through strong permitted transitions to the levels of interest. These additional levels are included only in the work of SZL and that of Liedahl (2000).

To attempt to determine the relative importance of these two effects, we reduced the size of the model atom from 130 levels to 13 (the number of levels in the $3p^6$ and $3p^53d$ configurations), but still used the new collision strength data. This has the effect of removing the cascade effects while retaining the effects of resonances on the collision rates between the levels of the $3p^53d$ configuration. At a density of $10^{11}\,cm^{-3}$, the $\lambda 241.7/\lambda 244.9$ line intensity ratio then rises by a factor of about 2 (to 0.1) compared with the full model, but is still a factor of 4 below the value obtained with the atomic data of Fawcett & Mason (1991). This would suggest that a factor of 4 in the ratio comes about from resonance effects, while a further factor of 2 arises from cascade contributions.

The importance of cascade effects has been recently demonstrated by Liedahl (2000), whose model atom includes 1067 states. His results (Fig. 3) also lead to significantly lower electron densities from the $\lambda 241.7/\lambda 244.9$ intensity ratio than in any previous work. The intensity ratio found by Liedahl (2000) is only a factor of 2.3 larger than that derived from the atomic data of SZL, based on collisional rates that do not include resonances, suggesting that resonance effects in the cross-sections are of less importance than cascading, in contradiction to our earlier conclusion that resonance effects are the more important. The most likely explanation for this contradiction is that the two processes are not independent insofar as they determine level populations.

5 CONCLUSIONS

The effect of resonance processes between the levels of the excited $3p^53d$ electron configuration has been shown to be important in determining the intensity ratios of the main diagnostic lines of Fe IX. In addition, we confirm the conclusion of Liedahl (2000) that cascade processes, particularly those involving the doubly excited $3p^43d^2$ electron configuration, are also important, although the relative magnitude of the two effects is uncertain. Together, these two effects reduce the densities derived from the $\lambda 241.7/\lambda 244.9$ intensity ratio by almost a factor of 10 (for high-density regions) compared with those derived from earlier atomic data, and bring them into much better agreement with those derived from lines of other ions. The opinion of Feldman (1992), that errors in the atomic data were unlikely to be large enough to explain discrepancies of such a magnitude, has been shown to be unfounded.

ACKNOWLEDGMENTS

The present collaboration benefited from visits to Meudon by PJS in 1998, 1999 and 2000, with support provided by the Observatoire de Paris and by the Université Paris 7. The hospitality of the Observatoire de Paris was much appreciated.

REFERENCES

Bar-Shalom A., Klapisch M., Goldstein W. H., Oreg J., 1998, The HULLAC code for atomic physics, unpublished
Behring W. E., Cohen L., Feldman U., 1972, ApJ, 175, 493
Berrington K. A., Burke P. G., Butler K., Seaton M. J., Storey P. J., Taylor K. T., Yu Y., 1987, J. Phys. B, 20, 6379
Berrington K. A., Eissner W., Norrington P. H., 1995, Comput. Phys. Commun., 92, 290
Brickhouse N. S., Raymond J. C., Smith B. W., 1995, ApJS, 97, 551
Cowan R. D., 1981, The Theory of Atomic Spectra. Univ. California Press, Los Angeles, CA
Dere K. P., Mason H. E., Widing K. G., Bhatia A. K., 1979, ApJS, 40, 341
Drake J. J., Laming J. M., Widing K. G., 1995, ApJ, 443, 393
Eissner W., 1991, J. Phys. IV, C1, 3
Eissner W., Seaton M. J., 1972, J. Phys. B, 5, 2187
Eissner W., Jones M., Nussbaumer H., 1974, Comput. Phys. Commun., 8, 270
Fawcett B. C., Mason H. E., 1989, At. Data Nucl. Data Tables, 43, 245
Fawcett B. C., Mason H. E., 1991, At. Data Nucl. Data Tables, 47, 17
Feldman U., 1992, ApJ, 385, 758
Feldman U., Doschek G. A., Widing K. G., 1978, ApJ, 219, 304
Flower D. R., 1977, A&A, 56, 451
Garstang R. H., 1969, PASP, 81, 488
Haug E., 1979, ApJ, 228, 903
Hummer D. G., Berrington K. A., Eissner W., Pradhan A. K., Saraph H. E., Tully J. A., 1993, A&A, 279, 298
Laming J. M., Drake J. J., Widing K. G., 1995, ApJ, 443, 416
Liedahl D. A., 2000, in Bautista M. A., Kallman T. R., Pradhan A. K. eds, Atomic Data Needs for X-ray Astronomy: Proceedings (http://heasarc.gsfc. nasa.gov/docs/heasarc/atomic)
Malinovsky M., Heroux L., 1973, ApJ, 181, 1009
Nussbaumer H., Storey P. J., 1978, A&A, 64, 139
Opacity Project Team, 1995, The Opacity Project, Vol. 1. IOP Publishing, Bristol
Opacity Project Team, 1996, The Opacity Project, Vol. 2. IOP Publishing, Bristol
Oreg J., Goldstein W. H., Klapisch M., Bar-Shalom A., 1991, Phys. Rev. A, 44, 1750
Saraph H. E., 1970, Comput. Phys. Commun., 1, 232
Saraph H. E., 1972, Comput. Phys. Commun., 3, 256
Thomas R. J., Neupert W. M., 1994, ApJS, 91, 461
Young P. R., Landi E., Thomas R. J., 1998, A&A, 329, 291

This paper has been typeset from a TEX/LATEX file prepared by the author.